

(p,n) Threshold-Curve Shapes and Measurements of Threshold Energy with H_1^+ Beams

R. O. BONDELID AND E. E. DOWLING WHITING*

Nucleonics Division, U. S. Naval Research Laboratory, Washington, D. C.

(Received 26 December 1963)

Yield curves have been calculated for (p,n) threshold reactions and the results have been applied to data previously obtained with the two-meter electrostatic analyzer at the Naval Research Laboratory. Taken into account in the calculation are the finite beam-energy spread from the analyzer, Doppler broadening due to thermal motion of the target nuclei, and the effect due to the statistical nature of the energy loss of protons in the target. A comparison of the yield-curve shape when the cross section is proportional to the emitted neutron velocity and the yield-curve shape when there is a nearby resonance is made. There is a small but calculable difference between the extrapolated yield curve intercept and true threshold energy. The threshold energies for several reactions are determined from data previously reported: $T^3(p,n)He^3$, 1019.76 ± 0.51 keV; $Li^7(p,n)Be^7$, 1881.27 ± 0.94 keV; $C^{13}(p,n)N^{13}$, 3237.1 ± 1.6 keV.

I. INTRODUCTION

ABSOLUTE measurements of the energy of bombarding particles in the low MeV region have been made with increased precision over the past several years.¹⁻⁴ Improved techniques for measuring the parameters of instruments used in determining the energy of bombarding particles have been of great importance in reducing the uncertainty in energy values. Improvements in target preparation techniques and improvement in target handling, especially during bombardment, have contributed to increased precision of measurements.

With increased precision of the instrumentation, methods of interpretation of the data obtained from a given experiment have assumed greater importance. Methods of interpretation of (p,γ) resonance reaction data have been dealt with by groups at the Naval Research Laboratory⁵ and at the University of Wisconsin.⁶ Carefully measured experimental yield curves exhibited some "anomalous" behaviors which required more sophisticated methods of analysis than were previously used. To obtain reasonable agreement in shape between the observed yield curves and calculated yield curves it was necessary to include in the theoretical treatment the effect of fluctuations in energy lost by the incoming particles. The energy loss distribution curves of Landau⁷ and Symon⁸ were used in the NRL

treatment of the problem. As a logical extension of the (p,γ) analysis, we have considered the effect of fluctuations in energy loss on (p,n) threshold reactions.

II. THE (p,n) CROSS SECTION NEAR THRESHOLD

If there is no resonance near threshold it is expected that the cross section for neutron emission is proportional to the velocity v of the neutron in the c.m. system. Conversely, neutron absorption is proportional to $1/v$ (the well-known $1/v$ law). (We are concerned only with those reactions in which S -wave neutrons are emitted.) Since the velocity of the neutron in the c.m. system is proportional to the square root of the difference between proton energy E_p and threshold energy E_{th} , it is expected that the cross section for neutron emission is proportional to $E^{1/2}$, where $E = (E_p - E_{th})$.

Newson *et al.*⁹ have discussed the case when there is a resonance near threshold and have given an analysis for the $Li^7(p,n)$ threshold. These authors give for the cross section near threshold when there is a nearby resonance the expression

$$\sigma(E_p) = \left(\frac{5}{8}\right)\pi\lambda_p^2 4\chi / [(1+\chi)^2 + 4(E_0 - E_p)^2 / \Gamma_p^2], \quad (1)$$

where $\chi = \Gamma_n / \Gamma_p$ and E_0 is the energy at resonance.

III. THE FORMAL YIELD EQUATION

A bombarding beam of protons having average energy E_b and energies E_i with a distribution represented by the function $g(E_b, E_i)$ is assumed to be incident on a target in which occurs a (p,n) threshold at energy E_{th} . The incident particles lose energy and at a depth x in the target particles with initial energy E_i have energies E_p with a distribution represented by the function $w(E_p, E_i, x)$. The particles will interact with the target nuclei with a probability for neutron production represented by the cross section $\sigma(E_p)$. The neutron yield is

* Present address: Frederick College, Portsmouth, Virginia.
¹ R. O. Bondelid and C. A. Kennedy, *Phys. Rev.* **115**, 1601 (1959); also NRL Report 5083, 1958 (unpublished).
² A. Rytz, H. H. Staub, and H. Winkler, *Helv. Phys. Acta* **34**, 960 (1961); A. Rytz, H. H. Staub, H. Winkler, and W. Zych, *Helv. Phys. Acta* **35**, 341 (1962).
³ E. H. Beckner, R. L. Bramblett, G. C. Phillips, and T. A. Eastwood, *Phys. Rev.* **123**, 2100 (1961).
⁴ B. R. Gasten, *Phys. Rev.* **131**, 1759 (1963).
⁵ R. O. Bondelid and J. W. Butler, *Phys. Rev.* **130**, 1078 (1963); also NRL Report 5897, 1963 (unpublished).
⁶ D. W. Palmer, J. G. Skofronick, D. G. Costello, A. L. Morsell, W. E. Kane, and R. G. Herb, *Phys. Rev.* **130**, 1153 (1963).
⁷ L. Landau, *J. Phys. (USSR)* **8**, 201 (1944).
⁸ K. R. Symon, Ph.D. thesis, Harvard University, 1948 (unpublished).

⁹ H. W. Newson, R. M. Williamson, K. W. Jones, J. H. Gibbons, and H. Marshak, *Phys. Rev.* **108**, 1294 (1957).

then given by the following expression:

$$Y(E_b, t) = n \int_{x=0}^t \int_{E_i=E_{th}}^{\infty} \int_{E_p=E_{th}}^{\infty} \sigma(E_p) g(E_b, E_i) \times w(E_p, E_i, x) dE_p dE_i dx, \quad (2)$$

where n is the number of target nuclei per unit volume and t is the target thickness in cm. This expression is identical to Eq. (1) of Ref. 5 except for the form of the cross section and the integration limits. We have taken the lower limit of the energy integrations as E_{th} because $\sigma=0$ for $E_p \leq E_{th}$. The determination of the functions $g(E_b, E_i)$ and $w(E_p, E_i, x)$ is discussed in detail in Ref. 5. The computer program used to evaluate Eq. (1) of Ref. (5) was modified so that Eq. (2) of this paper could be evaluated.

IV. EVALUATION OF THE YIELD EQUATION

If we assume a monoenergetic beam of incident protons, an energy loss dE/dx which is the same for all protons, and a thick target, Eq. (2) reduces to an integration of σ over the target thickness in units of energy loss and the limits of integration are from E_{th} to E_b . If we take σ proportional to $E^{1/2}$, where E is here defined as $(E_b - E_{th})$, the yield is proportional to $E^{3/2}$. Hence a plot of $Y^{2/3}$ versus E is a straight line whose intercept on the energy axis is E_{th} . If we include the effect of finite incident beam-energy spread, the resulting plot of $Y^{2/3}$ versus E exhibits a curvature near threshold, but an extrapolation which excludes this curvature also intercepts the energy axis at E_{th} . Consequently, those investigators who report neutron-threshold data have adopted the practice of plotting net yield (observed neutrons less background) to the $\frac{2}{3}$ power as a function of the average bombarding energy E_b and extrapolating the resulting straight-line portion to its intercept with the energy coordinate. This intercept is then taken to be the threshold energy.¹⁰ Because of the general usefulness of reporting threshold data using the described technique, the results of the calculations presented in this paper are in terms of the calculated yield raised to the $\frac{2}{3}$ power.

The $C^{13}(p,n)N^{13}$ Threshold

We chose this threshold as our first illustration because targets of C^{13} can be made which have a uniform composition and there is no resonance near the threshold energy. Figure 1 shows the general effect of fluctuations in energy loss on the $C^{13}(p,n)$ yield curve. Curve I was calculated with the assumption that the energy loss dE/dx is the same for all protons. Curve II was calculated using the distribution curves for energy loss as given by Symon⁸ and as discussed in Ref. 5. The target thickness assumed in the calculation was 8 keV and the beam-energy resolution was taken to be 0.01%.

¹⁰ J. B. Marion, Rev. Mod. Phys. 33, 139 (1961).

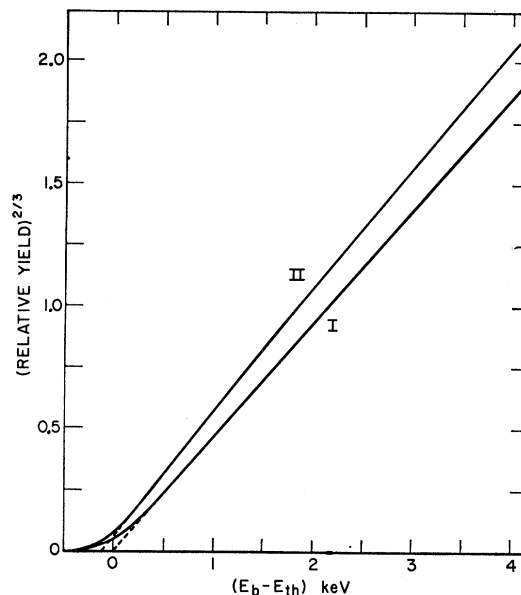


Fig. 1. Calculated yield curves for the $C^{13}(p,n)$ reaction for a target thickness of 8 keV and a beam-energy resolution of 0.01%, assuming $\sigma(E_p)$ proportional to $E^{1/2}$. Curve I: a uniform energy loss dE/dx assumed for all protons. Curve II: distribution curves given by Symon⁸ used for energy loss of protons in the target.

ever, the effective beam-energy spread is greater than this because of Doppler broadening due to thermal motion of the target nuclei which is included in the calculation. If it is assumed that the observed intercept is more realistically related to the intercept calculated by application of the energy loss distribution curves than to that intercept calculated from a uniform rate of energy loss then the observed intercept is lower than the true threshold energy. In the case shown in Fig. 1

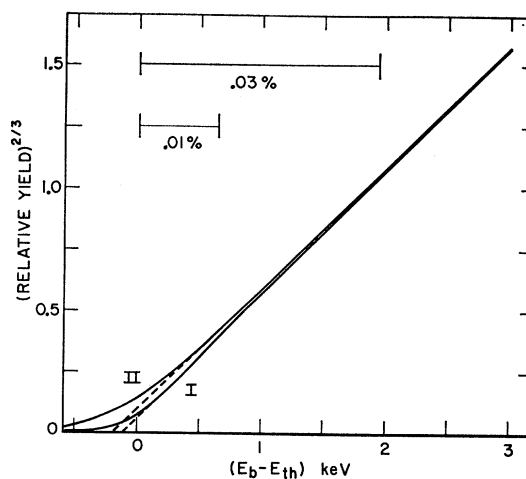


Fig. 2. Calculated yield curves for the $C^{13}(p,n)$ reaction for a target thickness of 8 keV, using the distribution curves of Symon.⁸ Curve I: beam-energy resolution, 0.01%. Curve II: beam-energy resolution, 0.03%. The total beam-energy spread due to the analyzer is shown for the two different resolutions.

the difference is 120 eV which is about 0.004% of the $C^{13}(p,n)$ threshold energy, 3.2371 MeV.

The effect of beam-energy spread is illustrated in Fig. 2. (In Fig. 2 and in subsequent figures the calculations include the energy spread due to finite analyzer resolution, Doppler broadening due to thermal motion of the target nuclei, and the energy loss distribution curves of Landau and Symon.) With a nominal analyzer resolution of 0.01% the total beam-energy spread from the analyzer alone is 640 eV, leading to an intercept 120 eV below threshold (curve I). With a nominal analyzer resolution of 0.03% the total beam-energy spread from the analyzer alone is about 2 keV, leading to an intercept 200 eV below threshold (curve II). The curves of Fig. 2 show that the intercept is lowered as the beam-energy spread increases. This indicates that for accurate threshold results one should compare the data with the calculated curve for the correct analyzer resolution. Other calculated curves (not shown) illustrate that the effect of finite beam-energy spread extends to values of $(E_b - E_{th})$ greater than shown in Fig. 2 with the result that the intercept energy is slightly increased as the range of extrapolation is increased. For the present example, if the range of extrapolation is 8 keV, and the nominal analyzer resolution is 0.03%, the intercept occurs at $(E_b - E_{th}) = -100$ eV, a difference of only 20 eV with the case illustrated in Fig. 2.

The $Li^7(p,n)Be^7$ Threshold

There is a strong resonance near threshold in this reaction, hence, the cross-section expression given by Eq. (1) should be used in calculating the yield curve. Because we are interested in the behavior of the yield curve in the immediate vicinity of threshold we make the approximation that $E \ll E_{th}$, or that $E_p \approx E_{th}$. Then λ_p^2 can be taken as a constant and $\Gamma_n/\Gamma_p = K(E/E_p)^{1/2} \approx E^{1/2}/C$, where $C = E_{th}^{1/2}/K$. The cross section then reduces to:

$$\sigma(E_p) = (\text{constant})E^{1/2} / [(1 + E^{1/2}/C)^2 + 4(E_0 - E_p)^2/\Gamma_p^2]. \quad (3)$$

The quantity K is taken from Ref. 9 to be ≈ 6 , hence $C \approx 7$ (keV) $^{1/2}$. The width of the resonance Γ_p was assigned the value 500 keV.⁹ The result for an assumed incident beam-energy spread of 0.01% and a pure target of LiF is shown in Fig. 3, curve I. Figure 3, curve II shows the result calculated when the cross section is assumed to follow the $E^{1/2}$ dependence. The two curves were normalized to have the same value at 1 keV because the results previously reported from this laboratory¹ were determined by extrapolation of the (net yield) data using a range of about 1 keV above threshold. If we assume a straight-line behavior of the (net yield) $^{2/3}$ curve for the correct cross section the intercept occurs 160 eV below threshold, but if we assume σ proportional to $E^{1/2}$ the intercept occurs 80 eV below

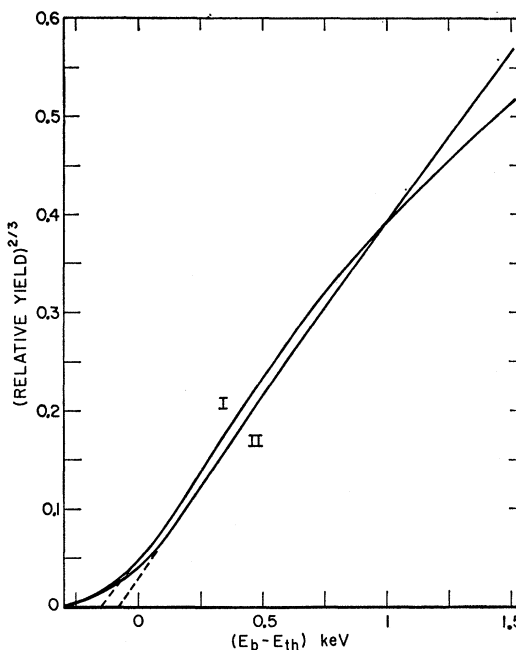


FIG. 3. Calculated yield curves for the $Li^7(p,n)$ reaction for a pure thick target of LiF and a beam-energy resolution of 0.01%, using the distribution curves of Symon.⁸ Curve I: $\sigma(E_p)$ given by Eq. (3). Curve II: $\sigma(E_p)$ proportional to $E^{1/2}$.

threshold. Clearly these results are dependent on the range of extrapolation used.

The $T^3(p,n)He^3$ Threshold

An experimental determination of this threshold has been reported by Bondelid *et al.*¹¹ The datum points shown in Fig. 4 are the same results reported in Ref. 11 and the line is the calculated yield based on the assumptions that (1) the target is a pure target composed of

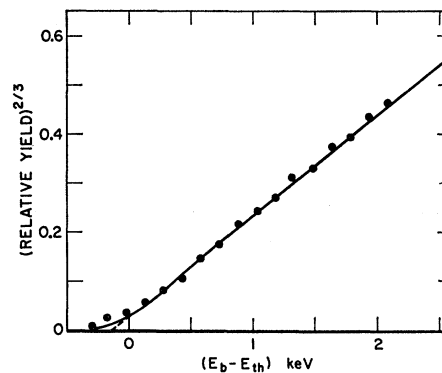


FIG. 4. Calculated yield curve and experimental data for the $T^3(p,n)$ reaction. The solid curve was calculated for a pure thick target of ZrF and a beam-energy resolution of 0.02%, assuming $\sigma(E_p)$ proportional to $E^{1/2}$. The datum points are the same results reported in Ref. 11.

¹¹ R. O. Bondelid, J. W. Butler, C. A. Kennedy, and A. del Callar, *Phys. Rev.* **120**, 887 (1960).

ZrT, (2) the beam-energy resolution is 0.02%, and (3) the cross section follows the $E^{1/2}$ dependence. The normalization procedure requires the slope and intercept of the straight line determined from a least-squares fit of the data to equal the slope and intercept of the straight line determined from the calculated yield. The intercept occurs 120 eV below threshold.

V. APPLICATION TO ENERGY CALIBRATION POINTS

The results of the present calculations show that it is reasonable when using a thick target to extrapolate (net yield)^{2/3} to the energy intercept; the energy value thus obtained can then be used as an energy calibration point. However, to obtain nuclear Q values, the small correction due to fluctuations in energy loss (though less than present experimental uncertainties, is systematic) should be made to the intercept value. In Table I we list several reactions for which the experimental results were previously obtained from the NRL two-meter electrostatic analyzer and have been reported.^{1,11} The first column lists the reaction, the second column shows the energy of the intercept, the third column shows the energy at threshold, the fourth column gives the Q of the reaction. The $\text{Li}^7(p,n)$ and the $\text{C}^{13}(p,n)$ threshold energies were originally reported from a linear extrapolation of the (net yield)¹ data. The present numbers listed in the table are determined from a direct comparison of the data with the calculated yield curves and hence contain the corrections discussed.

For calibration purposes the data from a threshold observation of the listed reactions can be compared with a yield curve calculated as described herein, in which event the threshold energies listed are the basis for the

TABLE I. Intercept energy, threshold energy, and Q values for the (p,n) reactions listed. These values are obtained from previously published data: $\text{T}^3(p,n)\text{He}^3$, Ref. 11; $\text{Li}^7(p,n)\text{Be}^7$ and $\text{C}^{13}(p,n)\text{N}^{13}$, Ref. 1.

Reaction	Intercept energy (keV)	Threshold energy (keV)	Q (keV)
$\text{T}^3(p,n)\text{He}^3$	1019.64 ± 0.51	1019.76 ± 0.51	-764.27 ± 0.37
$\text{Li}^7(p,n)\text{Be}^7$	1881.11 ± 0.94	1881.27 ± 0.94	-1644.79 ± 0.82
$\text{C}^{13}(p,n)\text{N}^{13}$	3236.9 ± 1.6	3237.1 ± 1.6	-3003.9 ± 1.5

TABLE II. The experimental conditions leading to the results shown in Table I.

Reaction	Target material	Analyzer resolution (percent)	Extrapolation range (keV)
$\text{T}^3(p,n)\text{He}^3$	ZrT	0.02	2
$\text{Li}^7(p,n)\text{Be}^7$	LiF	0.03	1
$\text{C}^{13}(p,n)\text{N}^{13}$	40% C^{13} , 60% C^{12}	0.03	3

calibration. The intercept energies listed can be used for calibration provided that the experimental conditions leading to the present results are duplicated. For convenience these experimental conditions are listed in Table II; the reaction, the target material, the analyzer resolution, and the range of extrapolation are given.

VI. FURTHER CONSIDERATIONS

Three additional factors which deserve some comment were considered in making the present calculations. (1) Calculations for thin targets indicate that one would expect to see a significant straight line portion in the (net yield)^{2/3} plot; however, the extrapolated intercept in the case of the $\text{C}^{13}(p,n)$ reaction can be as much as 300 eV below the threshold energy if the target is very thin, $t=50$ eV. Correspondingly smaller intercept errors result as the target thickness is increased. (2) Calculations were made for two different materials for the $\text{T}^3(p,n)$ threshold. In addition to ZrT, a target of solid T_2O was assumed. The intercept for the former target came at $(E_b - E_{th}) = -120$ eV while for the latter target the intercept appeared at $(E_b - E_{th}) = -90$ eV. (3) A contaminating layer of average energy loss 50 eV was assumed to be covering a target of C^{13} and the yield curve was calculated, with the result that the intercept was shifted upward 50 eV from the intercept obtained with the pure target assumption.

ACKNOWLEDGMENTS

We are grateful to H. Hancock and the staff of the Research Computation Center of NRL for the programming and evaluation of Eq. (2). We would like to thank K. L. Dunning for continued encouragement.